The Brill Transition in Transcrystalline Nylon-66

ARTICLE *in* MACROMOLECULES · MAY 2006

Impact Factor: 5.8 · DOI: 10.1021/ma060487h

The Brill Transition in Transcrystalline Nylon-66

A. Y. Feldman,*,† E. Wachtel,‡ G. B. M. Vaughan,§ A. Weinberg,⊥ and G. Marom†

Casali Institute of Applied Chemistry, The Hebrew University of Jerusalem, 91904 Jerusalem, Israel; Chemical Research Infrastructure Unit, The Weizmann Institute of Science, 76100 Rehovot, Israel; European Synchrotron Radiation Facility (ESRF), BP 220, 38043 Grenoble, France; and Shenkar College of Engineering and Design, 52526 Ramat-Gan, Israel

Received March 5, 2006; Revised Manuscript Received May 1, 2006

ABSTRACT: The Brill transition in transcrystalline nylon-66 occurs at a temperature that is 15 K higher than in the parent spherulitic nylon-66. This difference is assigned to the high level of crystalline orientation and chain packing order in the former. The similarity of the influence of the orientated morphology on the Brill transition and on the glass transition is pointed out, suggesting that the Brill transition, which is inherently a first-order process, comprises a second-order element. Utilizing the brightness of the synchrotron microbeam WAXD to make in situ diffraction measurements during relatively rapid heating and by running two consecutive cycles at different heating rates, the activation energy for the Brill process is derived for the first time. The values of 77 and 28 kJ/mol are calculated for transcrystalline and spherulitic nylon-66, respectively.

Introduction

The Brill transition in polyamides was discovered originally in 1942 in nylon-66, showing that a reversible polymorphic phase transition, from the triclinic (α-phase) to the pseudohexagonal structure, occurs at 162 °C. Although the transition point is sharp, it is preceded by gradual crystallographic changes, occurring over a relatively wide temperature range and entailing dimensional changes of the triclinic crystallographic unit cell. These changes are easily monitored by wide-angle X-ray diffraction (WAXD) performed as a function of temperature, showing gradual changes in the diffraction pattern, wherein the room temperature spacings—0.44 nm (d_{100}) and 0.37 nm ($d_{010/110}$)—are shifted to lower and higher values, respectively. Above the transition the two diffraction maxima are replaced by one with a spacing of 0.42 nm.[1−4] The arithmetic difference between the two *d* spacings of the triclinic cell (designated the index of chain packing, ICP),[5] as a function of temperature, can be extrapolated to zero to determine T_B, the temperature of the Brill transition.

Over the years since its discovery, the Brill transition has been observed and studied in other types of polyamides in addition to nylon-66 to determine the influence of numerous factors, such as the material parameters, crystallization conditions, and thermal history. It has been found that T_B depends strongly on the crystallization conditions, and for nylon-66 it varies between 139 and 230 °C.[1−24] In particular, for crystallization from the melt, the higher the crystallization temperature, the higher the observed T_B, with T_B values of ∼160−225 °C reported for nylon-66 crystallized between 196 and 260 °C.[6] For nylon-66 crystallized from a range of solvents and crystallization temperatures, T_B values of ∼200−220 °C have been reported.[7−9] As the transition is reversible, the pseudohexagonal phase of nylon-66, which crystallizes above T_B, reverts to the higher density triclinic structure on cooling below T_B.[6,10] It is noted that T_B on heating is higher than that on cooling (hysteresis). Also, it has been observed that the Brill transition varies among even−even[9−15] and odd−even polyamides.[16] Different experimental tools have been employed to investigate the Brill transition, including X-ray diffraction methods,[1−13] NMR,[17,18] DSC,[6,19−21] IR,[20−22] FTIR,[14,15,22,23] synchrotron SAXS,[24] and dilatometric measurements.[25]

Despite numerous studies, the nature of the Brill transition is still quite controversial. Ramesh et al.[6] claim that the hysteresis exhibited by the Brill transition upon heating and cooling reflects a first-order process. However, an endothermic peak at T_B can very rarely be identified in DSC traces, with the exception of crystallization from solution.[6,8,19] Also, the birefringence of spherulitic nylon-66 does not undergo any significant change in passing through the Brill transition region.[26]

In comparison to the widely published studies on the Brill transition in polyamides, there are few publications on the Brill transition in polyamide reinforced/filled composites.[27,28] In one example, the transition was studied in montmorillonite/nylon-66 composites by high-temperature WAXD. The T_B of the composite was 10 K higher than that of the neat nylon-66.[28] However, to the best of the authors' knowledge, no one has studied the Brill transition in transcrystalline (tc) composite materials nor how crystallite orientation in general affects the Brill transition.

For a number of years now we have been involved in a wide spectrum study of transcrystallinity in a variety of composite materials, a field which has recently been reviewed by Quan et al.[29] Our original research on tc layers in nylon-66 composites[30] comprised a detailed crystallization kinetics study under both isothermal and nonisothermal conditions, which set the transcrystallization conditions used thereafter in our subsequent research, including the current paper. In one of our earlier papers on the effect of nucleating agents and fibers on the crystallization of nylon-66[31] it is shown that under isothermal conditions at 250 °C the induction time for transcrystallization on Kevlar 49 fiber is shorter than 250 s, and its growth rate at 248.5 °C is 0.75 μm/min (0.60 μm/min at 250 °C[30]). Moreover, it is shown by hot-stage microscopy that even unnucleated nylon-66 (the same as used in the present study) develops a significant spherulitic structure already after 30 min at 248 °C. Furthermore, another reference showed that after a 3 h isothermal crystallization at 250 °C followed by ice−water quenching of a

† The Hebrew University of Jerusalem.
‡ The Weizmann Institute of Science.
§ European Synchrotron Radiation Facility.
⊥ Shenkar College of Engineering and Design.

10.1021/ma060487h CCC: $33.50
Published on Web 06/01/2006

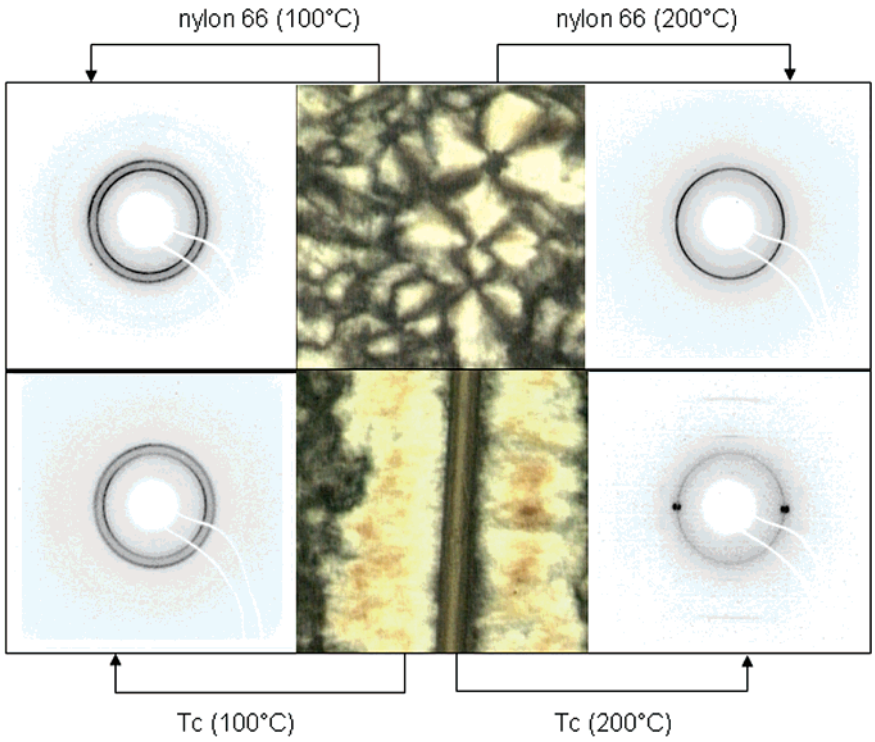

Figure 1. Polarized optical photos and 2D WAXD images of nylon-66 and transcrystalline nylon-66 below and above the Brill temperature.

multifilament microcomposite the transcrystalline layer invaded the whole matrix space between the fibers, leaving no space for any bulk crystallization to occur during the quenching stage.[32] Consequently, 3 h isothermal crystallization at 250 °C has been the procedure of choice in most of our subsequent studies of tc layers in nylon-66 composites[33−36] on which synchrotron microbeam WAXD studies were performed to analyze the orientation distribution of the crystallites[37] and its effects on mechanical properties.[38]

Recently, a new set of in situ synchrotron microbeam measurements has allowed us to investigate the Brill transition during melting and crystallization of transcrystalline and filled nylon-66, and the results are reported below.

Experimental Section

Materials. Nylon-66 pellets were obtained from Nilit, Israel (M_w = 325 000 and M_n = 16 800). Aramid fibers Kevlar-49 (Du-Pont 1420 denier yarn) and chopped aramid fibers Kevlar 29 (3 mm long, Du-Pont) were used as reinforcement.

Sample Preparation. *Extrusion*. Melt blending of neat nylon-66 and nylon-66 with 1%-wt of aramid chopped fibers was carried out in a twin-screw microcompounder (DSM, Netherlands). Blending/mixing was performed at 290 °C for a period of 10 min followed by extrusion/drawing at 250 °C of 350 μm diameter filaments.

Transcrystallinity. Microcomposites of nylon-66 reinforced by aramid fibers and displaying a transcrystalline layer were prepared according to the procedure published in (ref 37). This procedure, which comprised a 3 h isothermal treatment at 250 °C followed by ice−water quenching, was expected to generate most of the tc during the isothermal step.[30−32] Visual examination of the composites was recorded by a Nikon polarized optical microscope (POM).

In Situ WAXD and DSC Measurements. Synchrotron microbeam wide-angle X-ray diffraction (WAXD) measurements were performed at the European Synchrotron radiation Facility (ESRF) on the Materials Science Beamline (ID-11). The X-ray beam was monochromatized at a wavelength of λ = 0.5436 Å and collimated to dimensions 2 μm (vertical) by 50 μm (horizontal). The exposure time for each sample varied from 10 to 20 s. Samples were inserted into 0.5 and 1 mm diameter Li-glass capillaries (with the sample long axis parallel to that of the capillary) and mounted in the hot stage (Linkam Scientific Instruments, THMS600, Waterfield, UK). The distance between the sample and the detector was set at ∼143 mm.

Each sample was scanned during two consecutive heating−cooling cycles from 100 to 270 °C and from 100 to 200 °C performed at 15 and 25 K/min, respectively. Readings were taken at either 5 or 10 K intervals.

Differential scanning calorimetry (DSC) was carried out in a Mettler DSC-30 calorimeter, at a heating rate of 10 K min^{-1}. The weight of each sample was about 6−8 mg.

The one-dimensional diffraction profiles were calculated from the 2D X-ray diffraction patterns using the image analysis programs Fit2D (ESRF, Dr. Hammersley) and Polar (SUNY, Stony Brook, NY).

Results

POM images of the original nylon-66 and the aramid fiber-based transcrystallinity are shown in Figure 1. This figure also presents the corresponding 2D WAXD images below and above T_B, used for the detection of the Brill transition. The common features in the diffraction patterns are the clear 100 and the 010/110 diffraction rings (of the triclinic phase) below T_B and the "shifted 100" diffraction ring (of the pseudohexagonal phase) above it, for both samples. The apparent differences are that the tc samples show sharp equatorial fiber diffraction[37] and that the diffraction rings of the nylon-66 matrix display an anisotropic intensity distribution, reflecting crystalline orientation in the tc layer below as well as above T_B. The latter point is important as it corresponds to a gradual process that is based on lattice spacing changes rather than gross morphological changes.

Using a series of such 2D diffraction patterns obtained during in situ measurements, the data have been analyzed to produce 3D representations of the diffraction profiles as a function of temperature. The results for the two materials (as in Figure 1) are presented in Figure 2 for a full heating−cooling cycle, as

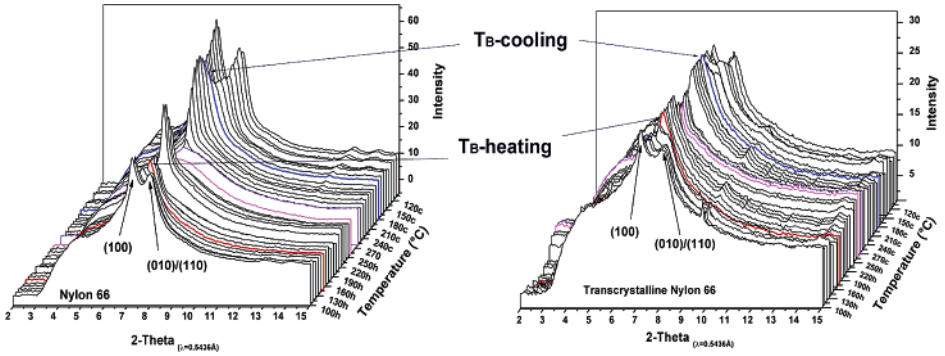

Figure 2. Three-dimensional representation of X-ray diffraction profiles of nylon-66 (left) and transcrystalline nylon-66 (right) during heating−cooling cycle (100 → 270 → 100 °C).

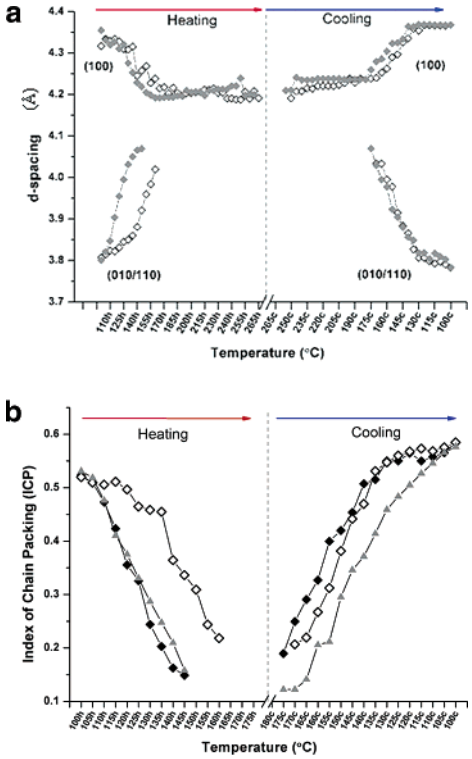

Figure 3. (a) Temperature dependence of d_{100} and $d_{010/110}$ spacings during a full heating−cooling cycle: ◆, nylon-66; ◇, transcrystalline nylon-66. (b) ICP during a full heating−cooling cycle: ◆, nylon-66; ◇, transcrystalline nylon-66; ▲, chopped aramid fibers−nylon-66.

denoted by arrows: T_B-heating to the melting point, T_B-cooling (in this order).

The values of T_B can be determined by measuring the *d* spacings for the 100 and 010/110 diffraction maxima (Figure 3a), followed by plotting ICP against temperature and extrapolating the linear regions to ICP equals zero, as shown in Figure 3b. With respect to these plots, two significant observations can be made: T_B-heating of nylon-66 (154 °C) is lower than that of tc nylon-66 (169 °C), while T_B-cooling is almost identical for the two materials (∼180 °C). The actual T_B values for two consecutive heating−cooling cycles are displayed in Table 1. It is noted that T_B-cooling is higher than T_B-heating (opposite to the hysteresis observed in the literature[6]) and that the samples which were heated to 270 K and cooled at 15 K/min exhibited T_B values of ∼180 °C in the second heating. The observation that in the first cycle T_B-cooling is higher than T_B-heating might be explained by the fact that in the first cycle cooling was performed directly from the melt without a preceding isothermal crystallization treatment. Indeed, after the second heating run to 200 °C (below the melting point) the common hysteresis was observed. The observation that the T_B-heating values in the second cycle were ∼180 °C is attributed to a higher heating rate of 25 K/min, utilized below to calculate the activation energies.

We attribute the difference in the T_B-heating values of the tc and nylon-66 materials to the high level of crystalline orientation and chain packing order, which are typical of the morphology of the former material as compared with the random nature of the spherulitic morphology. This argument for the higher T_B-heating of the tc material is supported by another observation regarding the ICP; i.e., the slope of the initial part of the curve is more moderate for the tc material than for the nylon-66. This is indicative of a slower reorganization of lateral chain packing (more gradual Brill transformation) of the former as compared to the latter, which can be taken to represent the rigidity of the orientated compact tc structure.

Because T_B is also sensitive to the thermal treatment,[6] a DSC comparison was required for the two materials. Figure 4 presents DSC traces measured upon heating of the two as-received materials, showing close resemblance in the main features. Both materials melt at the same temperature of ∼263 °C with similar melting enthalpies of ∼65 J/g, confirming that the different thermal treatments of the two samples have nevertheless resulted in the same degree of crystallinity. It is noted that the small endothermic peak (solid-state crystallization) that precedes the melting of the nylon-66 material amounts to ∼2 J/g, but this is considered to be negligible.

To verify the conclusion that the difference between the tc and nylon-66 materials is a reflection of the orientated compact structure of the former and is not due to another filler effect that ought to be accounted for, additional measurements were made with chopped aramid fiber-filled nylon-66 composites. This system which was extruded at 250 °C and cooled spontaneously to RT did not show any tc, indicating further the crucial role of the isothermal treatment at 250 °C for transcrystallization. The DSC thermograms in Figure 4 show that the melting point of this material and its melting enthalpy are very similar to those of the nylon-66 parent material.

Regarding the Brill transition of the chopped fiber composite, Figure 5 presents X-ray diffraction profiles for this composite in the same 3D format as in Figure 2. The values of T_B-heating and cooling for the two heating cycles, determined using the temperature dependence of ICP (Figure 3b) as described above, are presented in Table 1. The results underline the similarity between the chopped aramid fiber−nylon-66 composite and the parent nylon-66 material, corroborating the claim that the different behavior of the tc material is derived from its compact orientated morphology.

Table 1. T_B Values for the Consecutive Heating−Cooling Cycles

	first heating (15 °C/min)	first cooling (15 °C/min)	second heating (25 °C/min)
nylon-66	154	180	185
chopped aramid fibers−nylon-66	157	182	178
transcrystalline nylon-66	169	178	180

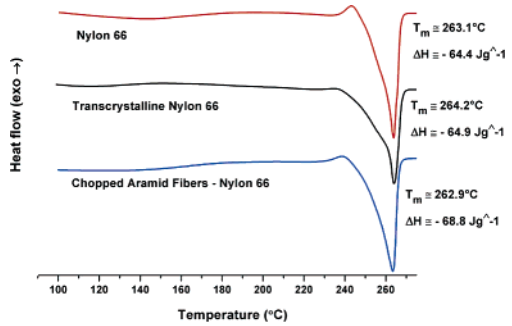

Figure 4. DSC traces of the as-received samples.

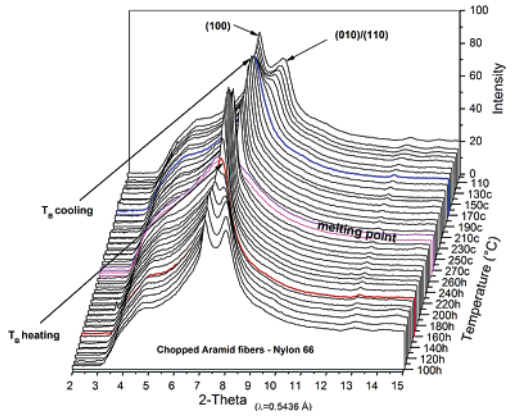

Figure 5. Three-dimensional presentation of X-ray diffraction profiles of chopped aramid fibers−nylon-66.

Discussion

The differences associated with the Brill transition between the transcrystalline and spherulitic nylon-66 can be accounted for by the crystallinity (e.g., crystal size and perfection—the intracrystalline explanation) and/or by the intercrystalline amorphous phase (the intercrystalline explanation). With reference to our previous work on tc in nylon-66 composites we note that the only significant difference between the tc and spherulitic structures is in the lamellar orientation and packing (which have been analyzed by synchrotron microbeam WAXD to determine the orientation distribution of the crystallites[37]) and not in the crystalline structure parameters (e.g., crystal size and lamellar thickness). This difference is reflected neither in the kinetics (rate) nor in the thermodynamics (melting point and enthalpy) of trans- and bulk crystallinity,[31] which is also the case here with melting point and degree of crystallinity identity of tc and spherulitic nylon-66 (Figure 4). This is an indication that the size and perfection are not an issue with respect to the effect of tc on the Brill transition. Conversely, we have strong evidence of significant differences between effects of trans- and bulk crystallinity on the interlamellar amorphous phase and related processes. For example, whereas high-density polyethylene (HDPE) does not exhibit a β-transition at all, an outstanding one is observed in tc HDPE.[39,40] Moreover, as discussed below, we have already presented clear evidence for the effects of tc on the glass transition, including in nylon-66. Hence, we argue that the results here align with the intercrystalline explanation.

The apparent paradox that on one hand the Brill transition is a first-order process taking place in the crystalline phase and on the other hand the tc affects the intercrystalline amorphous phase can be resolved as follows. Considering that the Brill transition is a first-order process, an explanation of the effect of the tc layer on the transition must be based on the existence of reciprocal interactions between the crystalline and amorphous phases. Indeed, it has been demonstrated unequivocally by other investigators, who performed SAXS measurements to study the Brill transition in nylon-66, that structural changes within the crystalline domains in the lamellae (as in the Brill transition) are accompanied by changes in the packing of the amorphous chain segments outside the lamellae.[24]

Overall, the results here portray a coherent picture in which the difference in the T_B-heating values for the tc and nylon-66 materials is assigned to the high level of crystalline orientation and chain packing order in the former. Moreover, the similarity between the effect of the orientated compact structure of the tc layer on the glass transition and the Brill transition cannot be disregarded. In a number of previous studies we investigated the effect of transcrystallinity on the glass transition in similar aramid fiber reinforced nylon-66 composites. We discovered by dynamic mechanical analysis[33] and dielectric spectroscopy analysis[41] that in the presence of tc this process is notably more restrained: tan δ is significantly smaller, its location is shifted to a slightly higher temperature, and its activation energy increases from 156 to 184 kJ/mol, all indicating that tc suppresses the chain mobility in the amorphous domains due to higher crystalline order. Concerning the Brill transition, the effect of the orientated compact structure of the tc layer is so dominant that it is active even in the rubbery state, some 100 K above T_g, which is evident from the ICP trends in Figure 3b.

In principle, in view of the fact that the Brill transition also comprises changes in the density of the interlamellar amorphous phase, an apparent resemblance between T_g and T_B might be anticipated. Thus, because of the time/temperature equivalence in viscoelastic materials different heating rates can be applied, resulting in different T_B values. Then, via an Arrhenius-type equation

$$w = Ae^{-\Delta E/RT} \tag{1}$$

(where w is the heating rate and T is the corresponding T_B), the activation energy (ΔE) of the Brill transition in the amorphous phase can be calculated. In retrospect, it appears that we have not utilized the full power of the in situ synchrotron facility with its ability to take rapid measurements as a function of temperature (neglecting the relatively short measurement time of 10−15 s at each temperature step). Still, in this work we have performed two consecutive heating−cooling cycles for each sample, the first at 15 K/min and the second at 25 K/min, and with the reservation that after the in situ cooling stage the tc layer is not fully regenerated (although the WAXD patterns show a high level of crystalline orientation) we attempt to estimate the activation energies. The calculated values (based on eq 1, with the data from Table 1) are 28, 41, and 77 kJ/mol—for the parent nylon-66, the chopped aramid fiber-nylon-66 composite and the transcrystalline nylon-66, respectively. It is obvious that the activation energy of the Brill transition due

to transcrystallinity is a factor of 2 higher than that of the transition in the nonorientated spherulitic material.

Conclusions

The Brill transition in nylon-66 is a first-order process, reflecting changes in the lateral chain packing in the crystalline phase upon change in temperature. In fiber-reinforced nylon-66 composites, the temperature at which the transition takes place is affected by the orientated compact structure of the transcrystalline layer, when this is present. The mechanism of this effect depends on the reciprocal interactions between the crystalline and amorphous phases, wherein structural changes within the crystalline domains in the lamellae are accompanied by changes in the interlamellar amorphous phase, and vice versa. Thus, the constraining effect of transcrystallinity on the Brill transition is similar to that observed previously for the glass transition: the Brill transition is shifted to higher temperature as compared with that of the nonorientated spherulitic material. Also, the activation energy of the corresponding process in the amorphous phase is 2-fold higher for the transcrystalline layer.

Acknowledgment. This research was supported by the Israel Science Foundation (Grant 69/05).

References and Notes

(1) Brill, R. *J. Prakt. Chem.* **1942**, *161*, 49.
(2) Brill, R. *Z. Phys. Chem.* **1943**, *1353*, 61.
(3) Sandeman, I.; Keller, A. *J. Polym. Sci.* **1956**, *19*, 401.
(4) Slichter, W. P. *J. Polym. Sci.* **1956**, *35*, 77.
(5) Simal, A. L.; Martin, A. R. *J. Appl. Polym. Sci.* **1998**, *68*, 453−474.
(6) Ramesh, C.; Keller, A.; Eltink, S. J. E. A. *Polymer* **1994**, *35*, 2483−2487.
(7) Starkweather, H. W., Jr.; Whitney, J. F.; Johnson, D. R. *J. Polym. Sci., Part A* **1963**, *1*, 715−723.
(8) Starkweather, H. W., Jr.; Jones, J. A. *J. Polym. Sci., Polym. Phys. Ed.* **1981**, *19*, 467.
(9) Jones, N. A.; Atkins, E. D. T.; Hill, M. J.; Cooper, S. J.; Franco, L. *Polymer* **1997**, *38*, 2689−2699.
(10) Jones, N. A.; Atkins, E. D. T.; Hill, M. J. *Macromolecules* **2000**, *33*, 2642−2650.
(11) Jones, N. A.; Atkins, E. D. T.; Hill, M. J.; Cooper, S. J.; Franco, L. *Macromolecules* **1996**, *29*, 6011−6018.
(12) Jones, N. A.; Atkins, E. D. T.; Hill, M. J.; Cooper, S. J.; Franco, L. *Macromolecules* **1997**, *30*, 3569−3578.
(13) Jones, N. A.; Atkins, E. D. T.; Hill, M. J. *J. Polym. Sci., Part B: Polym. Phys.* **2000**, *38*, 1209−1221.
(14) Li, W.; Huang, Y.; Zhang, G.; Yan, D. *Polym. Int.* **2003**, *53*, 1905−1908.
(15) Huang, Y.; Li, W.; Yan, D. *Eur. Polym. J.* **2003**, *39*, 1133−1140.
(16) Cui, X.; Yan, D. *Eur. Polym. J.* **2005**, *41*, 863−870.
(17) Hirshinger, J.; Miura, H.; Gardner, K. H.; English, A. D. *Macromolecules* **1990**, *23*, 2153−2169.
(18) Murthy, N. S.; Curran, S. A.; Aharoni, S. M.; Minor, H. *Macromolecules* **1991**, *24*, 3215−3220.
(19) Xenopoulos, A.; Wunderlich, B. *Colloid Polym. Sci.* **1991**, *269*, 375−391.
(20) Yoshioka, Y.; Tashiro, K.; Ramesh, C. *Polymer* **2003**, *44*, 6407−6417.
(21) Yoshioka, Y.; Tashiro, K. *Polymer* **2003**, *44*, 7007−7019.
(22) Vasanthan, N.; Murthy, N. S.; Bray, R. G. *Macromolecules* **1998**, *31*, 8433−8435.
(23) Cooper, S. J.; Coogan, M.; Everall, N.; Priestnall, I. *Polymer* **2001**, *42*, 10119−10132.
(24) Murthy, N. S.; Wang, Z. G.; Hsiao, B. S. *Macromolecules* **1999**, *32*, 5594−5599.
(25) Won, J. C.; Fulchiron, R.; Douillard, A.; Chabert, B.; Varlet, J.; Chomier, D. *J. Appl. Polym. Sci.* **2001**, *80*, 1021−1029.
(26) Magill, J. H. *J. Polym. Sci., Part A* **1966**, *4*, 243−265.
(27) Eersels, K. L. L.; Groeninckx, G.; Koch, M. H. J.; Reynaers, H. *Polymer* **1998**, *39*, 3893−3900.
(28) Zhang, Q. X.; Yu, Z. Z.; Yang, M.; Ma, J.; Mai, Y. W. *J. Polym. Sci., Part B: Polym. Phys.* **2003**, *41*, 2861−2869.
(29) Quan, H.; Li, Z. M.; Yang, M. B.; Huang, R. *Compos. Sci. Technol.* **2005**, *65*, 999−1021.
(30) Klein, N. Transcrystallinity Phenomenon and its Influence on the Properties and Performance of Thermoplastic Composites. Ph.D. Thesis, The Hebrew University of Jerusalem, 1995.
(31) Klein, N.; Selivansky, D.; Marom, G. *Polym. Compos.* **1995**, *16*, 189−197.
(32) Klein, N.; Marom, G.; Pegoretti, A.; Migliaresi, C. *Composites, Part A* **1995**, *26*, 707−712.
(33) Klein, N.; Marom, G. *Composites, Part A* **1994**, *25*, 706−710.
(34) Klein, N.; Marom, G.; Wachtel, E. *Polymer* **1996**, *37*, 5493−5498.
(35) Nuriel, H.; Klein, N.; Marom, G. *Compos. Sci. Technol.* **1999**, *59*, 1685−1690.
(36) Feldman, A.; Gonzales, M. F.; Marom, G. *Macromol. Mater. Eng.* **2003**, *288*, 861−866.
(37) Feldman, A. Y.; Gonzalez, M. F.; Wachtel, E.; Moret, M.; Marom, G. *Polymer* **2004**, *45*, 7239−7245.
(38) Feldman, A. Y.; Wachtel, E.; Zafeiropoulos, N. E.; Shneider, K.; Stamm, M.; Davies, R. J.; Weinberg, A.; Marom, G. *Compos. Sci. Technol.*, in press.
(39) Pegoretti, A.; Ashkar, M.; Migliaresi, C.; Marom, G. *Compos. Sci. Technol.* **2000**, *60*, 1181−1189.
(40) Alon, Y.; Marom, G. *Macromol. Rapid Commun.* **2004**, *25*, 1387−1391.
(41) Nuriel, H.; Kozlovich, N.; Feldman, Y.; Marom, G. *Composites, Part A* **2000**, *31*, 69−78.

MA060487H